

"Multispectral Image Data Fusion Using Projections onto Convex Sets Techniques"

MARCIA L. S. AGUENA¹, NELSON D. A. MASCARENHAS¹

¹UFSCAR - Universidade Federal de São Carlos, Via Washington Luís, Km 235, 13565-905 São Carlos, SP, Brazil
{aguena,nelson}@dc.ufscar.br

Abstract. The problem of image data fusion includes several techniques for data integration from different sensors about a given object. The process can be divided in two stages: (a) pixel interpolation on each observed image to equalize their resolutions; and (b) synthesis of the fused image using the interpolated images. This work proposes the use of projection onto convex sets (POCS) techniques in both stages of the image data fusion process: on the interpolation stage, by creating intermediate pixels more adapted to the local characteristics of the observed images; and on the synthesis stage, by generating a final multispectral image that incorporates the best spatial and spectral characteristics of the initial images. As an example, the algorithm is applied to Spot satellite images.

1. Introduction

The interpolation and the data fusion of images are techniques used for compatibility and integration of images, from different sensors, of the same object. The interpolation tries to equalize the spatial resolution of the different data sources, while the data fusion combines the data obtained in the previous step, by providing an image with the best characteristics of each combined image. In the case of remote sensing, multispectral images have good spectral resolution and panchromatic image have good spatial resolution so the data fusion process attempts to synthesize an image with the best characteristic of each original image.

There are several methods for image data fusion described in the literature. One group of methods is based on the IHS transformation, which is used in a large variety of works as in Haydn et al.[10] and Brum [03], who used the panchromatic and multispectral bands of the SPOT satellite to generate three synthetic bands with the resolution of the panchromatic band and ideal synthetic bands close to the original multispectral bands. Extensions of these ideas are based on linear projection techniques as Principal Components Analysis and Projection Pursuit, as in Byrne et al. [04], Orlando et al. [16] and Petrakos et al.[18].

The idea that in high-resolution multispectral images, the energy of the spectral features is concentrated in low frequencies and the energy of the spatial features (edges) is concentrated in high frequencies origins a large variety of methods as in Aiazzi [01], who combine interpolated multispectral images with a panchromatic band, subtracted of this low pass version, or using a multirate filter bank as in Ghassemian [05] and Bethume et al [02]. Following these steps, some works have applied the wavelet transforms techniques, as Gazerli e Soldati [06],

Núñez et al. [15], Scheunders [21], Gómez et al [07] (but merging multispectral and hyperspectral images).

Mascarenhas et al. [13] proposed the simulation of a degraded SPOT panchromatic band by linear combination of multispectral bands as an example of a potential method to decrease the data rate on the link between the satellite and the ground. Latter Mascarenhas et al. [14] proposed a new data fusion method using bayesian statistical estimation theory that uses the multispectral and panchromatic bands of SPOT satellite to generate ideal synthetic multispectral bands, close to 10x10m spatial resolution.

The use of local correlation coefficients for data fusion was proposed by Hill et al [11] and Zaniboni and Mascarenhas [23]. The latter method used locally adaptive correlation coefficients in the interpolation phase and, in the synthesis, a new method was proposed by performing a projection onto the linear subspace that defines the least squares solution of the synthesis problem.

This work explores the projections onto convex sets (POCS) methods both in the interpolation, for the definition of the locally adapted correlation coefficients, and in the synthesis, by projecting the interpolated images on the subspace of solutions.

1.1– Multispectral and Panchromatic Images

Multispectral images are obtained by sensors with narrow spectral bands, and for this reason, they have good spectral resolution. On the other hand, panchromatic bands have poor spectral resolution, but better spatial resolution. In this work, we will treat multispectral and panchromatic bands generated by the HRV sensor of the SPOT satellite, whose characteristics are presented in Table 1.

Type of Image	Band	Spectral Band (μm)	Spatial Resolution (m)
Panchromatic	1	0,51-0,73	10x10
Multispectral	1	0,50-0,59	20x20
	2	0,61-0,68	20x20
	3	0,79-0,89	20x20

Table 1 – SPOT image characteristics.

1.2 – Projections Onto Convex Sets

The POCS techniques have been applied to the solution of a wide variety of problems. As a rule, vector-space projections do not furnish “optimum” solutions such as those associated with minimum-mean square error, maximum entropy, maximum likelihood, maximum *a posteriori* estimation and others, but the projection methods, specifically convex projections methods, always yield a solution consistent with a set of constraints furnished by the user.

In its most general form, the practical application of a POCS method has the following framework: we want to recover, design or determine an unknown value using some information that is known in the form of constraints. The unknown value is treated as a vector in a Hilbert space, and the known constraints are described in the form of closed convex sets in this space. Without losing generality, assume that there are a total of m sets C_1, C_2, \dots, C_m available. Each set is usually associated with a single constraint although sometimes it is convenient to include multiple constraints in a single set. Then, the intersection of all these sets, say $C_0 = \bigcap_{i=1}^m C_i$, will contain all the possible solutions to the problem because each solution satisfies all the available information about the unknown. With the sets defined by projection equations called projectors, an initial value is successively projected on all constraint sets, until it converges to a value or arrives to a satisfactory solution [22].

2. Interpolation

The following method was proposed by Mascarenhas et al [14] and complemented by Zaniboni and Mascarenhas [23]. The POCS version of the method will be presented in section 3. Basically, we want to interpolate images of 20x20m resolution to make them compatible with images of 10x10m resolution. Both the pixel values on the original grid, as well as those on the interpolated grid, are regarded as random variables. The local linear estimation of the interpolated pixels is performed under the minimum mean square error criterion, by using the orthogonality principle [12]. For simplicity, the separability of the correlation structure on the spatial and the spectral

domains [11] is assumed. Furthermore, we also assume separability of the spatial correlation structure in the horizontal and vertical directions and a first order Markovian model in each direction. This assumption has also been widely used in the image processing literature [20].

A 3x3 neighborhood on each of the three 20m resolution multispectral bands (B1, B2 and B3) of the satellite image is used to linearly estimate four 10m resolution pixels covering the central pixel of the neighborhood on each band, as shown in Figure 1.

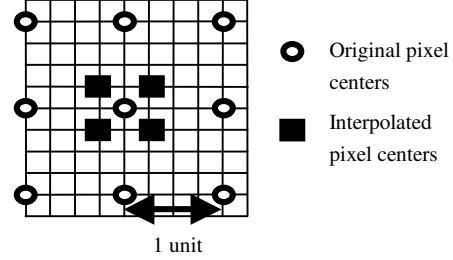


Figure 1 – Graphic representation of interpolation grid.

Therefore, we use 27 pixels (nine on each band) to estimate 12 pixels (four on each band). The vector obtained by lexicographically ordering the observations on the 3x3 neighborhood over the three multispectral bands, that is, ordering first by columns, then by rows and finally by bands, is denoted by the (27×1) vector y .

Let \hat{x} be the (12×1) vector obtained by a similar lexicographic ordering of the estimated pixels on the central 2x2 neighborhood over the three multispectral bands. So, the non-homogeneous linear estimator will have the form:

$$\hat{x} = Ay + b \quad (01)$$

Under a Bayesian approach for estimation, through the orthogonality principle [10], the matrix A and the vector b will be obtained by:

$$A = \sum_{xy} \sum_{yy}^{-1} \quad (02)$$

and,

$$b = E[x] - \sum_{xy} \sum_{yy}^{-1} E[y], \quad (03)$$

leading to,

$$\hat{x} = E[x] + \sum_{xy} \sum_{yy}^{-1} (y - E[y]) \quad (04)$$

where $E[x]$ is the statistical expectation, \sum_{xy} is the cross covariance matrix of x and y , and \sum_{yy} is the auto-covariance matrix of y . We adopt the physically reasonable assumption that, in the interpolated process, the expected values should not be modified, i.e.,

$$E[x] = E[y] \quad (05)$$

Under the separability assumption and lexicographic

ordering, the covariance matrices will be given by [2]:

$$\sum_{xy} = (C_h)_{xy} \otimes (C_v)_{xy} \otimes (\Sigma_s) \quad (06)$$

$$\sum_{yy} = (C_h)_{yy} \otimes (C_v)_{yy} \otimes (\Sigma_s) \quad (07)$$

The symbol \otimes represents the Kronecker product of two matrices and h, v and s represent, respectively, the horizontal, vertical and spectral directions. Observe that the Kronecker product does not commute, i.e., $A \otimes B \neq B \otimes A$ [03]. Therefore, depending on the order of the factors, different results could be obtained. However, the adopted lexicographic ordering by rows, columns and bands imposes the unique ordering given by equations (06) and (07) to represent the correlation structure between the involved pixel values.

Under the first order Markovian spatial correlation structure, the matrices $(C_h)_{xy}$ e $(C_h)_{yy}$ will be given by:

$$(C_h)_{xy} = \begin{bmatrix} \rho_h^{3/4} & \rho_h^{1/4} & \rho_h^{5/4} \\ \rho_h^{5/4} & \rho_h^{1/4} & \rho_h^{3/4} \end{bmatrix} \quad (08)$$

$$(C_h)_{yy} = \begin{bmatrix} 1 & \rho_h & \rho_h^2 \\ \rho_h & 1 & \rho_h \\ \rho_h^2 & \rho_h & 1 \end{bmatrix} \quad (09)$$

where ρ_h is the correlation coefficient on the horizontal direction. The same structure is valid for $(C_v)_{xy}$ and $(C_v)_{yy}$, by substituting ρ_h by ρ_v . The specification of the powers of ρ_h and ρ_v depends on the distance between pixel positions in the horizontal direction, by adopting the Markovian structure. It is implicitly assumed that the distance between adjacent pixels on the original multispectral bands is unity. The specification of the correlation coefficients allows an adaptation of the method to the image local characteristics.

The covariance matrix \sum_s is the covariance matrix between the multispectral bands and will be given by:

$$(\Sigma_s) = \begin{bmatrix} \sigma_{11}^2 & \sigma_{12}^2 & \sigma_{13}^2 \\ \sigma_{21}^2 & \sigma_{22}^2 & \sigma_{23}^2 \\ \sigma_{31}^2 & \sigma_{32}^2 & \sigma_{33}^2 \end{bmatrix} \quad (10)$$

where σ_{ji}^2 is the covariance between the bands i and j , and σ_{ii}^2 is the variance of the band i .

The covariance matrix of the (12x1) vector \hat{x} , that gives the interpolated pixels, is easily found:

$$\sum_{\hat{x}} = A \sum_{yy} A^T = \sum_{xy} \sum_{yy}^{-1} \sum_{xy}^T \quad (11)$$

where is A given by the equation:

$$A = \sum_{xy} \sum_{yy}^{-1} \quad (12)$$

It should be observed that the (12x12) covariance

matrix $\sum_{\hat{x}}$ carries not only spectral information, but also information about the interpolated pixels.

3. Correlation Coefficients

In Zaniboni e Mascarenhas [23], the technique of locally adapted correlation coefficients was used. The idea was to adapt the coefficients to local statistical changes of the image, using discrete higher values for ρ_h and ρ_v when the region presents lower local differences between the pixels and discrete lower values when the region presents higher local differences between the pixels. The values of ρ_h and ρ_v were used in equations (08) and (09).

The new method proposed in this paper can be described by the follow steps:

a) For every pixel $y_{i,j,n}$ with $i=1,\dots,I$, $j=1,\dots,J$, and $n=1,2$ e 3 (where i represents rows, j coluns and n the multispectral band) on the multispectral images that will be interpolated, the horizontal, $Sh_{i,j,n}$, and vertical, $Sv_{i,j,n}$, "sum of diferences" are computed over a 3x3 pixels neighborhood centered in $y_{i,j,n}$. This is the neighborhood that will be used in the interpolation process.

$$Sh_{i,j,n} = \sum_{a=-1b=0}^1 \sum_{b=0}^1 |y_{i+a,j+b-1,n} - y_{i+a,j+b,n}|, \quad (13)$$

$$Sv_{i,j,n} = \sum_{a=-1b=0}^1 \sum_{b=0}^1 |y_{i+a-1,j+b-1,n} - y_{i+a,j+b,n}|, \quad (14)$$

(b) The two-dimensional histogram of horizontal and vertical local roughness measures ($S_{h_{i,j,n}}$, $S_{v_{i,j,n}}$) is computed for all pixels of the three multispectral images.

(c) On this histogram, k two-dimensional centers are found $(Ch,Cv)_m$, $m = 1, \dots, k$, defining k regions by using the k-means clustering algorithm.

(d) In the interpolation process, for each $y_{i,j,n}$ neighborhood, with $n=1,2$ e 3, distances between the three local roughness measures, represented by the pairs $(Sh_{i,j,n}, Sv_{i,j,n})$ and k centers $(Ch,Cv)_m$ are computed, with $m=1,\dots,k$, as shown in Figure 2.

(e) The lowest distance of each center m is considered the error margin of center m , δ_m , described by equation (15) e illustrated by Figure 3:

$$\delta_m = \min_{n=1}^3 \left\| (Ch,Cv)_m - (Sh_{i,j,n}, Sv_{i,j,n}) \right\| \quad (15)$$

(f) Each center $(Ch,Cv)_m$ associated with the margin δ_m generates the set I_m , given by:

$$I_m = \left\{ (x_1, x_2) : \left\| (Ch,Cv)_m - (x_1, x_2) \right\| \leq \delta_m \right\} \quad (16)$$

and the projector P_{im} :

$$P_{im} = \begin{cases} (x_1, x_2) & \text{if } (x_1, x_2) \in I_m, \\ (Ch,Cv)_m + \left(\frac{(x_1, x_2) - (Ch,Cv)_m}{\left\| (x_1, x_2) - (Ch,Cv)_m \right\|} \right) \delta_m & \text{cc} \end{cases} \quad (17)$$

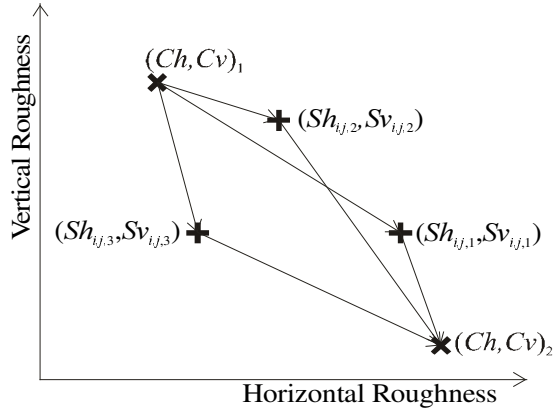


Figure 2 – Illustration of the distances calculation between the local differences $(Sh_{ij,n}, Sv_{ij,n})$ and k centers $(Ch, Cv)_m$ ($m=1$ and 2 in this example).

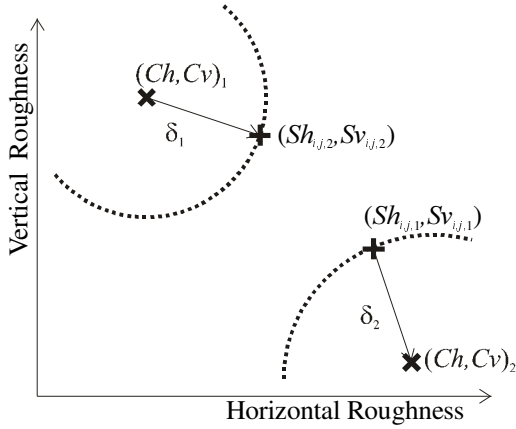


Figure 3 - Illustration of margin d_m calculation.

(g) The average of the points $(Sh_{ij,n}, Sv_{ij,n})$, for $n=1,2$ and 3 is chosen as initial value $(x_1, x_2)_0$, and the projection is made using a parallel POCS algorithm, in other words, the projections of these values onto the k sets I_m are calculated and the average is used as the answer of the iteration, new projections are made and a new average is calculated, until it converges for a value, called $(x_1, x_2)_f$.

(h) Using the value $(x_1, x_2)_f$, obtained on the previous step, a mapping function is calculated to find the ρ_v and ρ_h that will be used on the interpolation, so that high roughness measure values must be mapped to low values of ρ_v and ρ_h , and low roughness measure values must be mapped to high values of ρ_v and ρ_h .

$$(\rho_v, \rho_h) = (1, 1) - (x_1, x_2)_f \quad (18)$$

4. Synthesis

In the synthesis process, the POCS method for linear system solution substitutes the projection

method for the least squares method solution. Let us denote by y_i , with $i=1, \dots, 3$ the pixel vector of the three multispectral bands, with $20 \times 20m$ resolution, corresponding to a given multispectral pixel \mathbf{E} . Let us denote p_j , with $j=1, \dots, 4$ the four panchromatic image pixels values with $10 \times 10m$ resolution, corresponding the same multispectral pixel \mathbf{E} . Finally, let us denote by f_k with $k=1, \dots, 12$ the synthetic pixel values with $10 \times 10m$ resolution, four of them in each synthetic band, corresponding the same multispectral pixel \mathbf{E} , as shown in Figure 4.

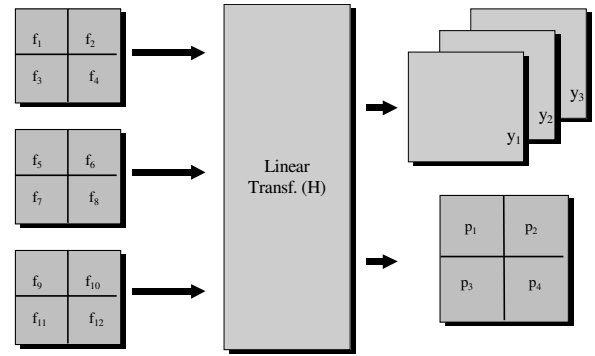


Figure 4 – Relationship between multispectral panchromatic and synthetic bands.

In the Bayesian synthesis process, the observation vector z is made up of seven components:

$$z^T = [p_1, p_2, p_3, p_4, y_1, y_2, y_3] \quad (19)$$

The vector f of synthetic pixels is made up by twenty-seven components:

$$f^T = [f_1 \dots f_{12}] \quad (20)$$

The vector f is locally related to the observed vector z by using an observation matrix H , to be described later, through a linear model, i.e.,

$$z = Hf \quad (21)$$

Since we wish to synthesize bands that are spectrally close to the multispectral bands, these synthetic bands are defined by ideal bands (vertical cutoffs) located over each one of multispectral Landsat bands B1, B2 and B3. Note that there is spectral overlap between the panchromatic band and the multispectral bands, as shown in Figure 5.

The components of each row of the matrix H are defined by the fraction of the area under the ideal synthetic spectral sensitivity curves. The spectral relative response curves for each sensor will define the parameters of the matrix H (see equations (23) and (24)).

More specifically, matrix H (12×27) is given in the form:

$$H = \begin{bmatrix} A_1 & A_2 & A_3 \\ B_1 & B_2 & B_3 \end{bmatrix} \quad (22)$$

where:

$$A_i = \begin{bmatrix} \alpha_i & 0 & 0 & 0 \\ 0 & \alpha_i & 0 & 0 \\ 0 & 0 & \alpha_i & 0 \\ 0 & 0 & 0 & \alpha_i \end{bmatrix} \quad (23)$$

and

$$B_i = \begin{bmatrix} \beta_{1i} & \beta_{1i} & \beta_{1i} & \beta_{1i} \\ \beta_{2i} & \beta_{2i} & \beta_{2i} & \beta_{2i} \\ \beta_{3i} & \beta_{3i} & \beta_{3i} & \beta_{3i} \end{bmatrix} \quad (24)$$

with $i=1, \dots, 3$ and

$$\alpha_i = \frac{P \cap S_i}{P}, \quad (25)$$

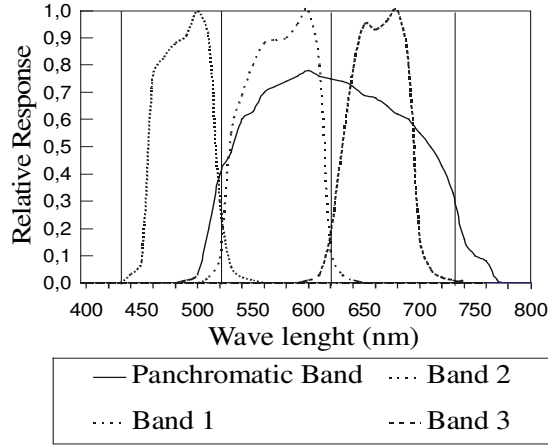


Figure 5 - Spot spectral curves.

where P is the area under the panchromatic band spectral response curve, S_i is the area under the ideal i^{th} band spectral response curve, $i = 1, 2, 3$, and $P \cap S_i$ is the area under the minimum of the panchromatic band spectral response curve and the ideal i^{th} band spectral response curve, $i = 1, 2, 3$, and,

$$\beta_{jk} = \frac{1}{4} \frac{x_{sk} \cap S_j}{x_{sk}}, \quad (26)$$

where x_{sk} is the area under the k^{th} multispectral band spectral response curve. The $x_{sk} \cap S_j$ is the area under the minimum of the k^{th} multispectral band spectral response curve and the ideal j^{th} band spectral response curve, $k = 1, 2, 3$ and $j = 1, 2, 3$. We make the assumption of an infinite spectral response of the ideal synthetic bands within their limits. The factor $1/4$ takes into account the different resolutions of the multispectral bands (20x20m) and the synthesized bands (10x10m).

The solution of equation (21) found using POCS methods is a linear system solution, in other words,

obtained by sequentially projecting the initial value onto sets, represented by the equations described by the rows of the H matrix, until arriving to a convergent value in the intersection of the constraint sets. The set S_i and the projector used for each H 's rows are given by the equations:

$$S_i = \{f : \langle H_i, f \rangle = z_i\} \quad (26)$$

$$P_{S_i} = \begin{cases} f, & \text{se } f \in S_i \\ f - \frac{\langle H_i, f \rangle - z_i}{\|H_i\|^2} H_i, & \text{otherwise} \end{cases}, \quad (27)$$

where H_i is the vector described by the i^{th} row of H matrix and z_i is the i^{th} element of vector z .

5. Experimental results

The experiments were made using images over São José dos Campos, SP, Brazil. Figure 6 shows the image of the original multispectral bands, with spatial resolution 20x20m and Figure 7 shows the image of the panchromatic band.



Figure 6 - Original Multispectral Bands

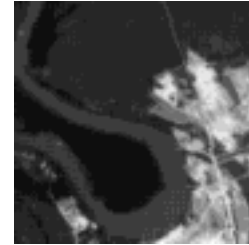


Figure 7 - Panchromatic Band

The interpolation process result is shown in Figure 8. The POCS method is iterative and the average of the number of iterations needed to converge for a result is in Table 2.

In the synthesis process, one of the factors that can influence the obtained image is the choice of the order of the rows of the matrix H that will be used for projection in the POCS method. This happens since the projector used in each row of matrix H (27), always provides the nearest vector to the initial value, and there is an infinite number of solutions, because the system of equations (21) is underdetermined. The result of projections with a normal order and inverse order of H rows, and as initial values the result of multispectral images interpolation is shown in Figure 9.

Maximum Error	Average Number of Iterations
10^{-4}	3,1496
10^{-5}	4,5139
10^{-6}	6,3328
10^{-7}	8,6162
10^{-10}	15,9616
10^{-20}	34,8097

Table 2 – Relationship between the tolerated maximum error and the average number of iterations to converge in the interpolation.

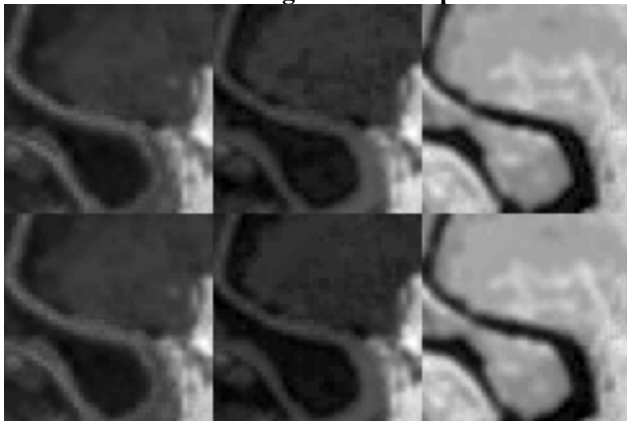


Figure 8 - Top to bottom: images resulting from bayesian and from POCS interpolation.

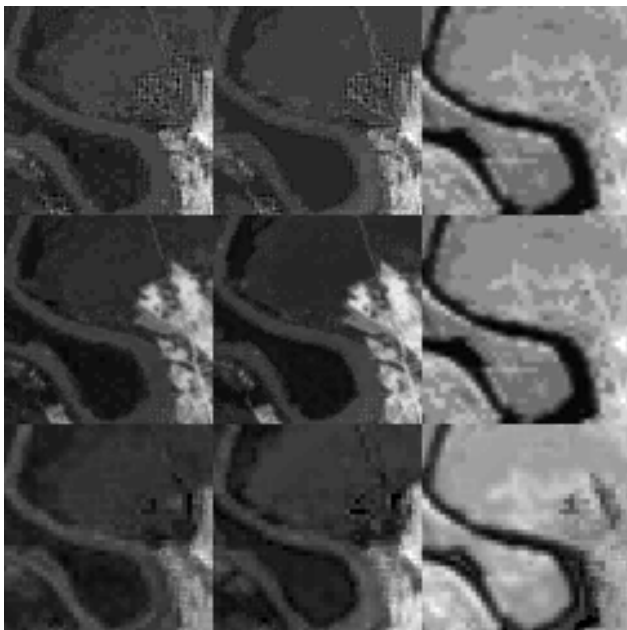


Figure 9 – Top to bottom, first the result of synthesis using projection on matrix H, synthesis using projection in inverse order of H and bayesian synthesis.

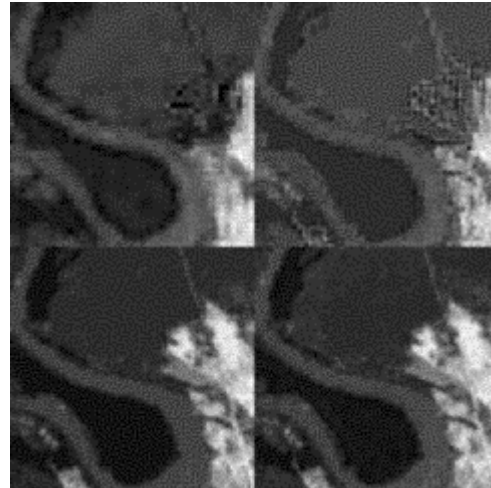


Figure 10 - Figure 12. Enlarged details: a) Multispectral original image of band 2 ; b) Panchromatic image; c) Projection in normal order; d) Projectio in reverse order .

We can better observe in the enlarged details in Figure 10, that the image projected using the normal order of the matrix H rows is closer to the original multispectral image (in the figure, enlarged with a 200% zoom.), and the projected image using the reverse order of the matrix H rows is closer to the panchromatic image. This happens because the first matrix H rows contain the restrictions of the panchromatic image with resolution $10 \times 10 \text{m}$ (sub matrices A_1 , A_2 and A_3), and the last lines contain the restrictions of the original multispectral images with resolution $20 \times 20 \text{m}$ (sub matrices B_1 , B_2 and B_3). The average number of iterations needed for the method to converge is 9,7164 for the normal order projection on matrix H rows, and 9,6201 for the reverse order projection on matrix H rows.

Acknowledgment

The work of Marcia Aguená was supported by a scholarship from CNPq.

References

- [01] Aiazzi, B., Alparone, L., Baronti, S., 2001, *Quality assessment of decision-driven pyramid-based fusion of high resolution multispectral with panchromatic image data*, Remote Sensing and Data Fusion over Urban Areas, IEEE/ISPRS Joint Workshop 2001 , Page(s): 337 –341
- [02] Béthume, S., Muller, F., Donnay, J., 1998, *Fusion of multispectral and panchromatic image by local mean and variance matching filtering techniques* Proceedings of The Second International Conference : Fusion of Earth Data : Merging Point Measurements,

- Raster Maps and Remotely Sensed Images. Sophia-Antipolis, France, 28-30 January pp. 31-36.
- [03] Brum, R. E., 1989, *Integration of the multispectral and panchromatic channels of the HRV (SPOT) sensor, for obtaining color composites with spatial resolution close to 10m*. MSc Thesis, (INPE-5035-TDL/403), INPE, São José dos Campos, S.P., Brazil (in portuguese).
- [04] Byrne, G.F., Crapper, P.F. and Mayo, K.K., 1980, *Monitoring land-cover change by principal component analysis of multitemporal Landsat data*, Remote Sensing Environment, 1, 887-888.
- [05] Candeias, A. L. B., 1992, *The use of Bayesian estimation theory on satellite data fusion*. MSc Thesis (INPE-5457-TDI/499), INPE, São José dos Campos, S.P. Brasil (in portuguese).
- [06] Garzelli, A., Soldati, F., 2001, *Context-driven image fusion of multispectral and panchromatic data based on a redundant wavelet representation*, Remote Sensing and Data Fusion Over Urban Areas, IEEE/ISPRS Joint Workshop 2001, Page(s): 122 – 126
- [07] Ghassemian, H., *Multi-sensor image fusion using multirate filter banks*, Proceedings. International Conference on Image Processing, 2001, Volume: 1, 2001 Page(s): 846 -849 vol.1
- [08] Gomez, R. B., Jazaeri, A., Kafatos, M., *Wavelet-based hyperspectral and multispectral image fusion*, 2001 SPIE's OE/Aerospace Sensing, Geo-Spatial Image and Data Exploitation II, Orlando, April 16-20, 2001.
- [09] Graybill, F. A., 1969, *Introduction to Matrices with Applications in Statistics*. Belmont, Wadsworth, pp. 196-221.
- [10] Haydn, R. Dalke, G.W. Henkel, J. Bare, J.C., 1992, *Application of the IHS color transform to processing of multisensor data and image enhancement in remote sensing of arid and semi-arid lands*, Proceedings of the 1st Thematic Conference of The International Symposium on Remote Sensing of Environment, Erim, Ann Arbor, Michigan, Cairo, Egypt, 19-25 January, pp. 599-616
- [11] Hill, J., Diemer, O., Stöver, Udelhoven, Th., *A local correlation approach for the fusion of remote sensing data with different spatial resolutions in forestry application*, International Archives of Photogrammetry and Remote Sensing, Vol. 32, Part 7-4-3 W6, Valadolid, Spain, 3-4 June, 1999.
- [12] Hunt, B.R., and Kübler, O., 1984, Karhunen-Loève multispectral image restoration, Part I: Theory. I.E.E.E. Transactions on Acoustics, Speech and Signal Processing, 32, 592-599.
- [13] Mascarenhas, N. D. A., Banon, G. J. F., and Fonseca, L.M.G., 1991, *Simulation of a panchromatic band by spectral linear combination of multispectral bands*. Proceedings of the International Geoscience and Remote Sensing Symposium, Espoo, Finland, June 1991 (New York. I.E.E.E.), pp. 407-414.
- [14] Mascarenhas, N. D. A., Banon, G. J. F., Candeias, A. L. B., 1996, *Multispectral image data fusion under a Bayesian approach*, International Journal of Remote Sensing, vol. 17, No. 8, pp. 1457-1471.
- [15] Núñez, J., Otazu, X., Fors, O., Prades, A., Palà, V., Arbiol, R., *Multiresolution-based image fusion with additive wavelet decomposition*, IEEE Transactions on Geoscience and Remote Sensing, Volume: 37 Issue: 3 Part: 1, May 1999
- [16] Orlando, J.R., Mann, R. and Haykin, S., 1990, *Classification of sea-ice images using a dual - polarized radar*, IEEE Journal of Oceanic Engineering, volume 15, pp. 228-237.
- [17] Papoulis, A., 1984, *Probability, random variables and stochastic processes*, Second Edition, New York, McGraw-Hill, pp. 407-414.
- [18] Petrakos, M., Dicarolo, W., Kanellopoulos, I., 1999, *Projection pursuit and a VR environment for visualization of remotely sensed data*, Proceedings of the International Geoscience and Remote Sensing Symposium, 1999. IGARSS '99 page(s): 2498 – 2500, vol.5.
- [19] Pratt, W. K., 1991, *Digital image processing*, Second Edition, New York: John Wiley.
- [20] *Proceedings of Data Fusion Systems Conference*, Johns Hopkins University Press, Naval Air Development Center, Warminster, PA, 1986-1994.
- [21] Scheunders, P., *Multispectral image fusion using local mapping techniques*, Proc. ICPR2000, International Conference on Pattern Recognition, Barcelona, Spain, september 3-8, (2000).
- [22] Stark, H, Yang, Y, 1998, *Vector space projections*, John Willey & Sons, New York.
- [23] Zaniboni, G. T.; Mascarenhas, M. D. A, *Fusão Bayesiana de imagens utilizando coeficientes de correlação localmente adaptáveis*, Anais de IX Simpósio Brasileiro de Sensoriamento Remoto, Santos, SP, 1998, CD-ROM :\sbsr\8_1350.pdf